Comparative Performance Analysis of Isolated and Non-Isolated DC-DC Converters with Solar PV Array for EVs Application

Rejaul Islam*, Md. Istianatur Rahman

Department of Electrical & Electronic Engineering, World University of Bangladesh, Avenue 6 Lake Drive Uttara Sector 17H, Bangladesh

*Corresponding author
doi: https://doi.org/10.21467/proceedings.123.5

ABSTRACT

Modern day's power electronics converters are very important for each and every electronic device such as portable devices, cell phones, laptop-computers, electric vehicles, etc. For the Electric Vehicles (EVs) the dc-to-dc converters are the best-suited and essential devices on account of their lightweight, high efficiency, smaller size, and high-power density, bi-directionality, reliability, cost-effectiveness. This paper provides a comparative study on non-isolated and isolated power dc-to-dc converters for EVs in which the main power source is PV (photo-voltaic) array module, in addition, a brief idea about design and calculation of passive components of power dc-to-dc isolated and non-isolated converters both in theoretically, and practically with simulation software. Here all the simulation results are tested by MATLAB simulation software and verified that the multi-phase multi-device interleaved boost dc-dc converter (MDIBC) is the best-suited candidate for both low and high power photo-voltaic based EVs due to their compact size, low cost, reliability, multifunctionality, bi-directionality, high efficiency, etc.

Keywords- DC-DC Converter, Electric Vehicles, PV Array, Duty Cycle.

1 Introduction

For centuries, human civilizations have been shaping through vehicles and continuously increasing their ranges more than a few localized societies. The advanced and modern forms of vehicular transportations are automobiles and these automobiles burn petrol, natural gas, or diesel for running and exhaust harmful components such as sulfur dioxide (SO2), oxides of nitrogen, and carbon dioxide (CO2). So, it is causing harm to human life and the environment due to the expanding usages of these traditional automobiles [1].

In the US, approximately 29% of greenhouse gas is emitted by the transportation sector which is shown in Fig. 1. On record, globally January 2020 was the hottest January according to the National Oceanic and Atmospheric Administration (NOAA), which is directly indicated to the emissions of GHG by humans. According to the Environmental Protection Agency's (EPAs) definition, emission sources of US greenhouse gas (GHG) can be divided into five sectors, namely: transportation (29%), industry (22%), electricity (28%), agriculture (9%), and commercial and residential (12%) [2].

Furthermore, the emission of greenhouse gas in the traditional automobile or vehicular industries had increased up to around 35 percentages from 1990 to 2010 while in the same time for other sectors it decreased by 15 percentages [3,4]. The replacement of traditional automobiles is gaining the most priority to stop this unwanted increase of GHG ambience and "Doha Amendment to the Kyoto

Proceedings DOI: 10.21467/proceedings.123; Series: AIJR Proceedings; ISSN: 2582-3922; ISBN: 978-81-954993-5-9

protocol (2012)" was signed in order to sustain the regulation. Due to these reasons, EVs are accepting as an excellent replacement for conventional vehicles [1, 3–6, 8].

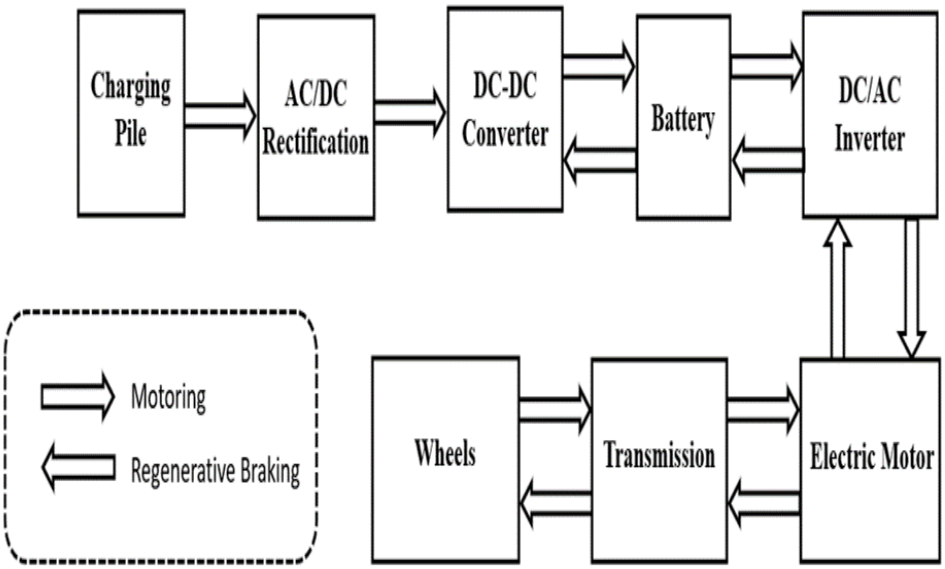

Fig. 1 EVs architectural block diagram.

Moreover, one or more storing-system (i.e., batteries and/or supercapacitors) is required in order to store the power from the output of the solar PV system and to drive the load of the electric vehicular system, hence it is one of the most essential components for EVs. Because, the PV system won't be able to supply power at night. Generally, the voltage level of the EVs load, EM (Electric Motor) is around 400-750V, and the voltage level of the PV system and the high voltage dc-bus for this paper is around 480-500V and around 550-600V respectively. On the other hand, available batteries and supercapacitors of the EV market is capable of storing around 250-360V and 150-400V voltages respectively. Thence, a stepping-down converter is required in order to charge the batteries and/or supercapacitors from high voltage dc-bus or/and PV array (i.e., during day-night operation) and a stepping-up converter is required for driving an EV. Furthermore, the converter steps up the dc voltage is known as the boost converter and whereas, the steps down operation of dc voltage is done by utilizing the buck Converter [7].

1.1 Isolated DC-DC Converters for PV system based EVs

This kind of power converters has three elementary operating steps and these are: DC/AC/DC. The first and last DC steps are the input and desired output voltage stages respectively and in order to increase the input lower voltage as well as to provide isolation from any uncertain fault an HFT (high-frequency transformer) is used in the interior stage. The most important issues in EVs are high-voltage gain and galvanic isolation which is provided by this intermediate HFT. In medium and high-power automobile appliances several categories of isolated dc-to-dc converters are utilized time and again [7]. Among them, isolated half-bridge converter (HBC) [9], and isolated full-bridge converter (FBC) [10] are often utilized in EV. The most compatible converter among these two converters is FBC because it helps power switching devices and diodes in the process of current-voltage stresses reduction, which

Proceedings DOI: 10.21467/proceedings.123
ISBN: 978-81-954993-5-9

Series: AIJR Proceedings
ISSN: 2582-3922

makes the FBC unique because it can't be found in other isolation boost converters. Furthermore, for simple architectural design and the lowest cost, the FBC has high overall system efficiency [7].

1.2 Non-Isolated DC-DC Converters for PV system based EVs

This kind of power converters are minimal in weight compared to the isolated converters because they do not contain any HFT for voltage gain. For medium and high-powered automobile appliances non-isolated converters are often used. There are several types of non-isolated power dc-to-dc converters such as buck-boost [12], boost [11], Cuk, etc. are available in the EV market [7,11,12]. Among them, non-isolation conventional boost converters (BC) are commonly utilized in EVs due to their positive gain of the output voltage, which is essential for an EM action. Moreover, the buck-boost converter is not suitable for vehicular applications because of the uncertain changing nature of its output current and the requirement of output voltage ripple filtering capacitor is large. Whereas, Cuk is only compatible for energy storage system (ESS), because they are kind of current-voltage-current converters, whereas an SC and/or a battery are the commonly used inputs in automobile equipment's [7]. Therefore, for positive low DC voltage gain (i.e., approximately less than four percentages) a conventional BC is best-suited [13].

2 DC-DC converters design

2.1 Boost DC-DC Converter (BC) design

A BC is a power converter, which increases or stepping-up level of the supplied dc voltage to a specified DC output voltage. The expression for passive component such as inductor and capacitor values of the BC are depicted as follows:

$$L = \frac{D \times V_{in}}{f_{sw} \times \Delta I_{lmax}}. \quad (1)$$

$$C = \frac{D \times I_{out}}{f_{sw} \times \Delta V_{out}}. \quad (2)$$

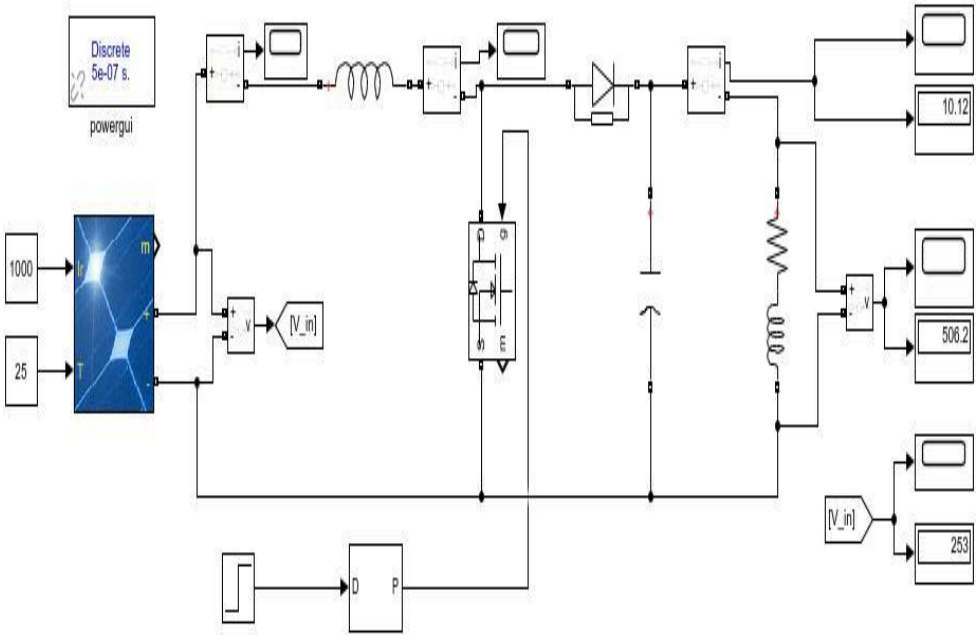

Fig. 2 MATLAB Simulation Circuit Diagram of BC.

2.2 Boost DC-DC Converter with Resonant Circuit (BCRC) design

There are mainly two types of soft-switching converter are available they are Zero Current Switching (ZCS) mode and Zero Voltage Switching (ZVS) mode. The BCRC can easily work both in ZCS and ZVS mode. Thus, the ZCS is achieved in the BCRC by opening and closing the main power switching device Q_1 and auxiliary power switching device Q_2 respectively, and vice-versa for the ZVS operating mode [14]. Moreover, the free-wheeling diode of the power switching device Q1 is started conducting every time prior to the close of the Q_1, hence the current becomes zero as a result increases the voltage and the converter operates as a conventional BC, as depicted in Fig. 3. By simply opening and closing the auxiliary power switching device Q_2, the BCRC can easily be achieved ZVC and ZCS respectively with the help of an auxiliary resonant circuit.

Furthermore, the equation of duty ratio for BCRC is the same as the conventional boost converter. So, the equations for designing the resonant inductor and capacitor are [14,15–17]:

$$L_r = \frac{V_{in} \times (V_{out} - V_{in})}{\Delta I_{lmax} \times f_{sw} \times V_{out}} . \quad (3)$$

$$C_r = \frac{D \times I_o}{f_{sw} \times \Delta V_{out}} . \quad (4)$$

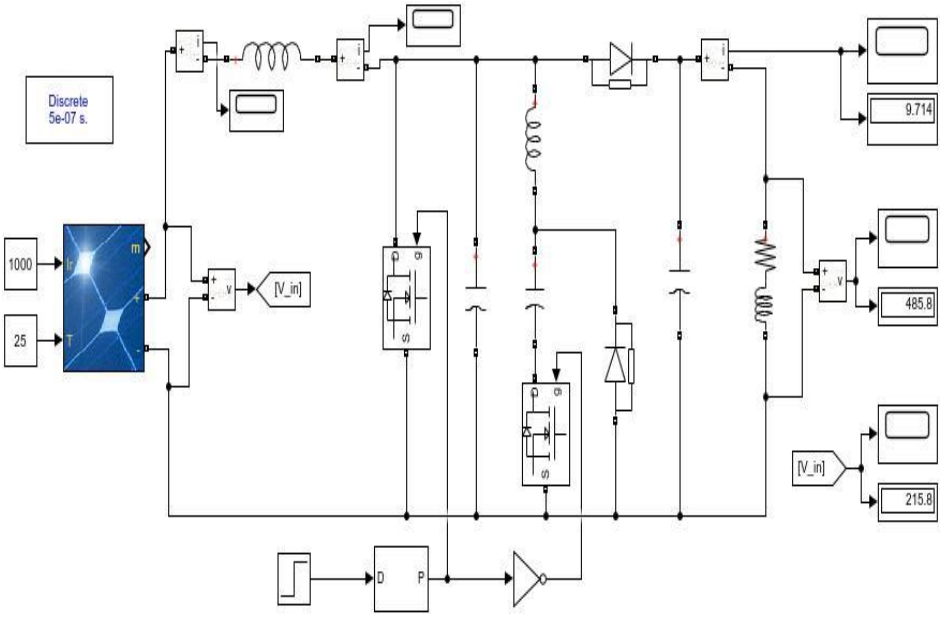

Fig. 3 MATLAB Simulation Circuit Diagram of BCRC

2.3 Isolated Full-Bridge Boost DC-DC Converter (FBC) design

Fig. 4 shows the simulation circuit diagram of FBC, which is composed of passive filtering elements (i.e., inductor and capacitor), an HFT for inverting operation, and a diode-based full-bridge rectifier in order to rectify the ac supply of HFT into dc output. The FBC has three working modes, they are:

i. CCM: Continuous Conduction Mode
ii. DCM: Discontinuous Conduction Mode and,
iii. Zero Inductor Current Mode.

Proceedings DOI: 10.21467/proceedings.123
ISBN: 978-81-954993-5-9

Series: AIJR Proceedings
ISSN: 2582-3922

Moreover, in order to terminate ripples from the input and output side of the HFT, inductor, and capacitor are utilized in the input and output side of the circuit respectively. In order to retain the output voltage of the FBC constant from a source whose power level changes over time (i.e., PV system), the PWM of the power switching-based inverting circuit differs via duty ratio in accordance with differing source.

The design equations of duty ratio (D) and passive components (L, and C) for FBC are considered in CCM. Thence, the equations for designing the D, L, and C of FBC can be written as,

$$D = \frac{V_{out}}{2n \times V_{in}} . \quad (5)$$

$$L = \frac{n \times D \times V_{out}}{2 \times \Delta I_{lmax} \times f_{sw}} . \quad (6)$$

$$C = \frac{D \times I_{out}}{f_{sw} \times \Delta V_{out}} . \quad (7)$$

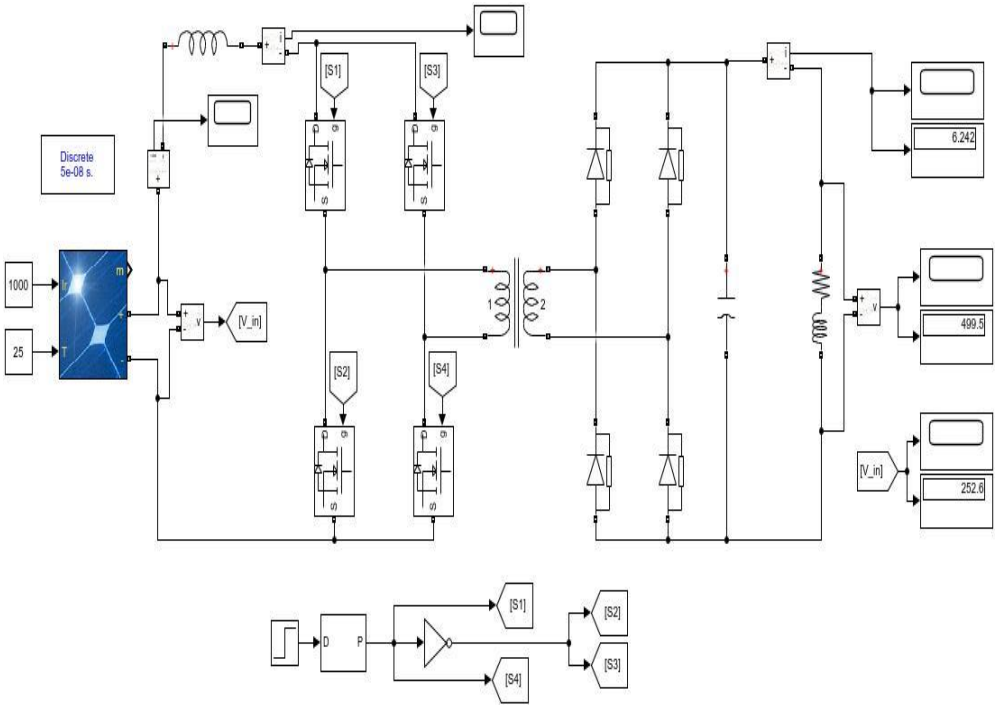

Fig. 4 MATLAB Simulation Circuit Diagram of FBC

2.4 Multi-Phase Interleaved Boost Converter (IBC) design

The multi-phase IBC in this paper has been designed for four-phase hence, it is consisting of four power switching devices, four inductors, and four power diodes, which is depicted in Fig. 5. Usually in IBC, the control scheme based on shifted phase is utilized in order to reduce the size of the filters (i.e., inductor, and capacitor), which is utilized for mitigating the current and voltage ripples. The ripples of the input current of the multi-phase IBC get reduced by distributing the input supplied current evenly among each boost/step-up level.

Moreover, the ripples of the supplied current can be mitigated easily by increasing the boost level/phases of the multi-phase IBC without changing the size of the previously available filtering components. Designing equations for the four-phase IBC are identical as the conventional BC. The equation for duty ratio of IBC converter is:

$$D = 1 - \frac{V_{in}}{V_{out}} . \quad (8)$$

Now, the equations for designing the passive filtering components such as, inductor (L) and capacitor (C) can be written as,

$$L = \frac{V_{out}}{4 \times f_{sw} \times N \times \Delta I_{lmax}} . \quad (9)$$

$$C = \frac{I_{lmax}}{4 \times f_{sw} \times N \times \Delta V_{out}} . \quad (10)$$

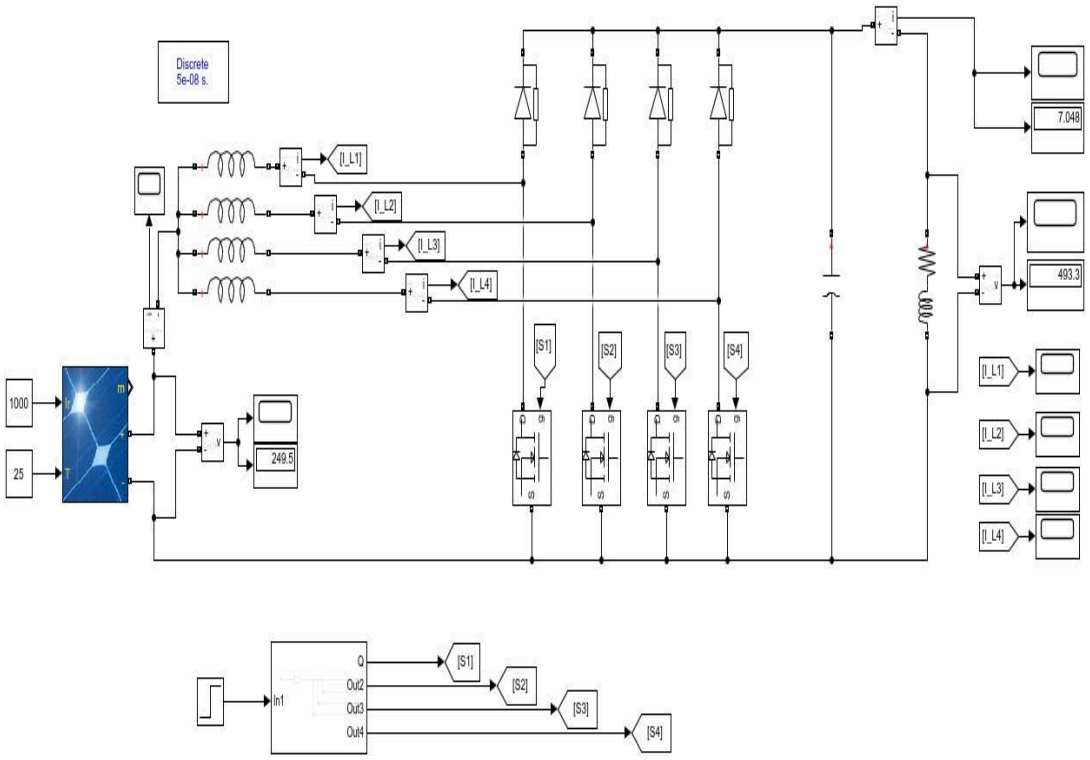

Fig. 5 MATLAB Simulation Circuit Diagram of Multi-Phase IBC.

2.5 Bidirectional Multi-Phase Multidevice Interleaved DC-DC Converter (MDIBC) design

The MDIBC converter simulation circuit diagram based on MATLAB software is illustrated in Fig. 6, which is consists of parallel switching devices per phase and an interleaving technique is used for connecting these parallel switching devices. Due to this interleaving technique, the per phase switching signals are transferred into 3600/(P×S). Here, P is the phase number and S is the parallel power switching device number per phase. Moreover, the ripples of the current and voltage are identic to (P×S) × $f_{sw\ ripple}$. Here, $f_{sw\ ripple}$ is the ripples due to the frequency of the switching devices.

Proceedings DOI: 10.21467/proceedings.123
ISBN: 978-81-954993-5-9

Series: AIJR Proceedings
ISSN: 2582-3922

As a result, the size of the heat mitigating component and passive components gets reduced by the amount of switching devices per phase compared to the conventional BCs. All the inductors in MDIBC are identical i.e., $L_1 = L_2 = L_3 = L_4 = L$ and all the switching devices has the identical duty ratio ($D_{PV1} = D_{PV2} = D$). So, the duty ratio of MDIBC can be calculated as:

$$D_{max} = \frac{1}{m}\left(1 - \frac{V_{in}}{V_{out}}\right) \quad . \quad (11)$$

and the design equations of inductor for both port and output filter capacitor of MDIBC are:

$$L = \frac{V_{out} \times (1 - mD) \times D}{N \times f_{sw} \times \Delta I_{lmax}} \quad . \quad (12)$$

$$C = \frac{D \times V_{out}}{R \times N \times \Delta V_{out} \times f_{sw}} \quad . \quad (13)$$

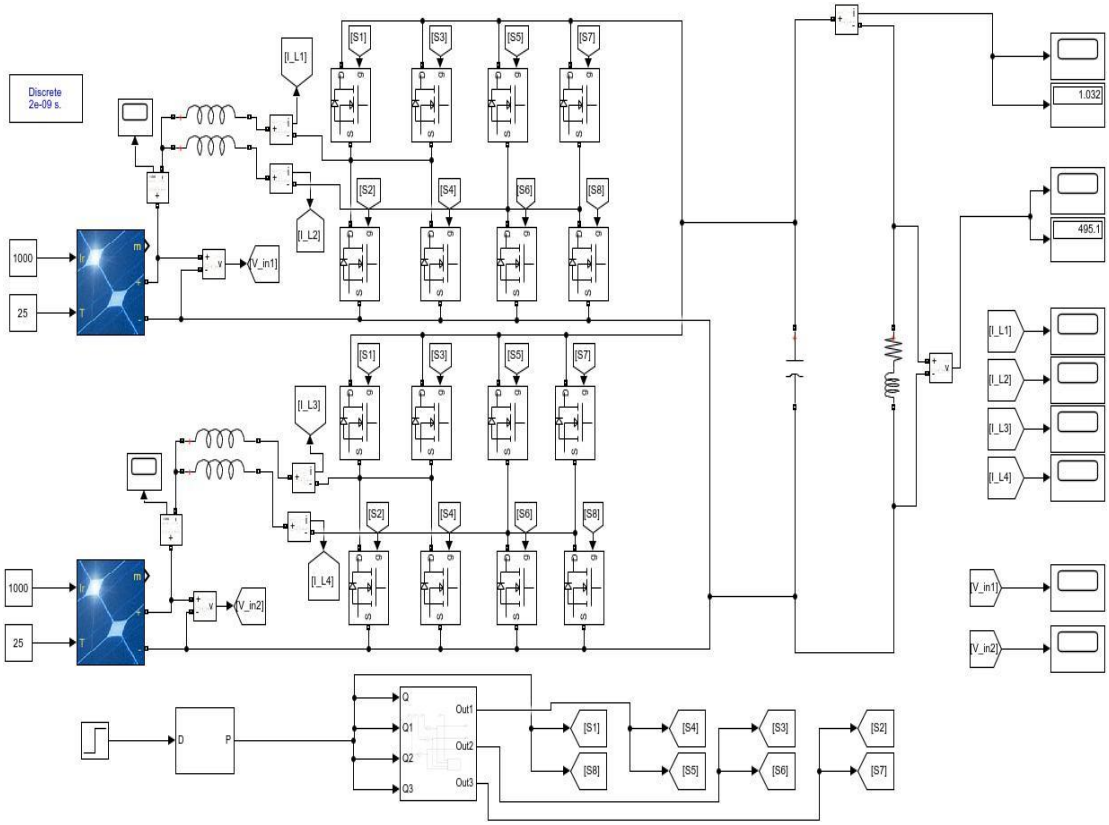

Fig. 6 MATLAB Simulation Circuit Diagram of MDIBC.

3 Results and Analysis

The values of the duty cycle and passive components (i.e., inductor and capacitor) are shown in Table-I, which are determined by using the classical design formulas. The parameters are specified in Table-I have taken from both the hardware and simulation models, which have been discussed above. In order to validate, calibrate, and parameterize the model of the power dc-to-dc converter, these design values are the most enlightened key. The illustrated converters efficiency map has been observed and the prototype is designed and tested based on these design values and specified parameters. The descriptions such as bandwidth, cut-off frequency, natural frequencies, and gain for linear reparation

have been mapped by utilizing these design values [7]. All the simulation is done with the help of MATLAB simulation software.

TABLE I. INPUT/OUTPUT CURRENT-VOLTAGE, PASSIVE COMPONENTS, AND OTHER DESCRIPTIONS VALUES FOR BOOST DC-DC CONVERTERS.

Parameters	BC	BCRC	FBC	IBC	MDIBC
Input voltage, V_{in} (V)	254	218	254	254	326, 254
Output voltage, V_{out} (V)	500	490	500	500	500
Switching frequency, f_{sw} (kHz)	30	30	30	30	20
Inductor current, I_{lmax} (A)	180	145.5	195	180	85
Max. ripples of current, ΔI_{lmax} (A)	7.2	5.82	7.8	7.2	3.4
Max. ripples of output voltage, ΔV_{out} (V)	10	9.8	10	10	10
Phase number	-	-	-	4	4
Output power P_0 (kW)	12.5	4.9	22	22	22
Max. duty ratio, D_{max}	50%	55%	50%	50%	50%
Inductor, L (µH)	588	6933	1068	144	42, 16
Capacitor, C(µF)	150	18	3.25	37.5	22

The simulation waveforms of input current, input voltage, inductor current, output current, and output voltage of BC are depicted in Fig. 7.

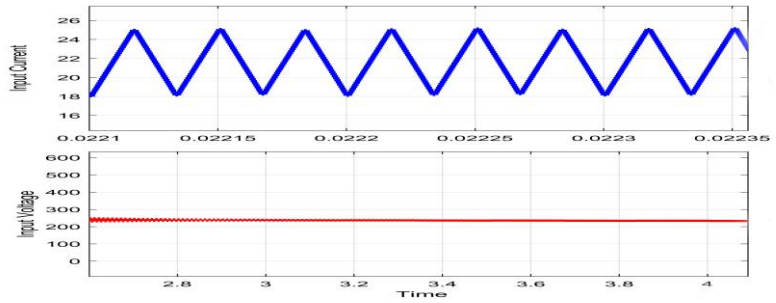

(a)

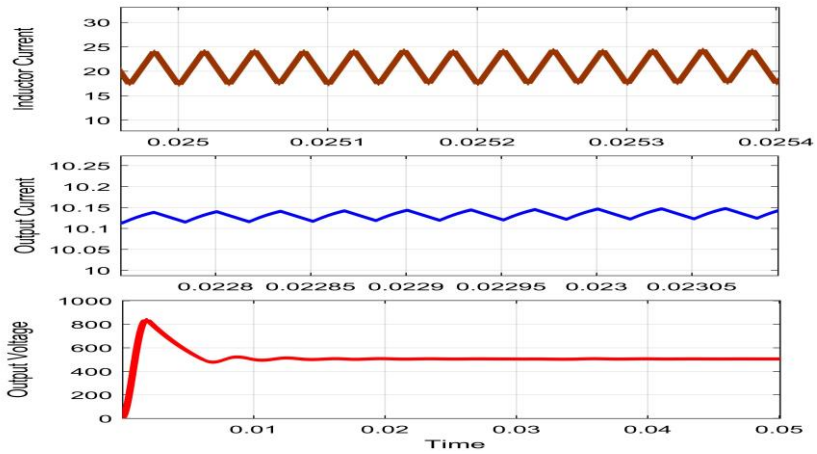

(b)

Fig. 7 Input-output waveforms of BC. (a) Waveforms of input current-voltage, and (b) waveforms of inductor current and output current-voltage.

Proceedings DOI: 10.21467/proceedings.123
ISBN: 978-81-954993-5-9

Series: AIJR Proceedings
ISSN: 2582-3922

The simulation waveforms of input/output current-voltage and the inductor current of BCRC are depicted in Fig. 8.

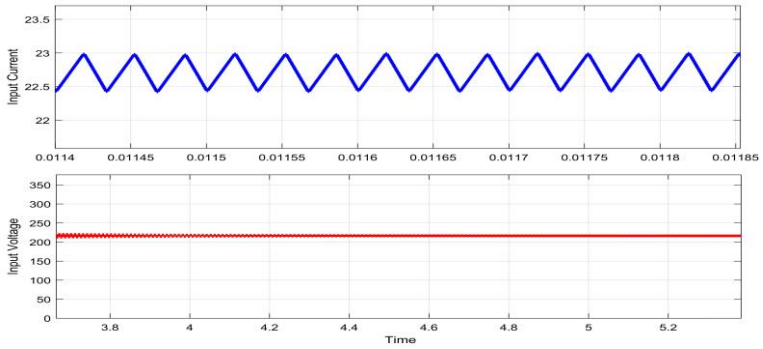

(a)

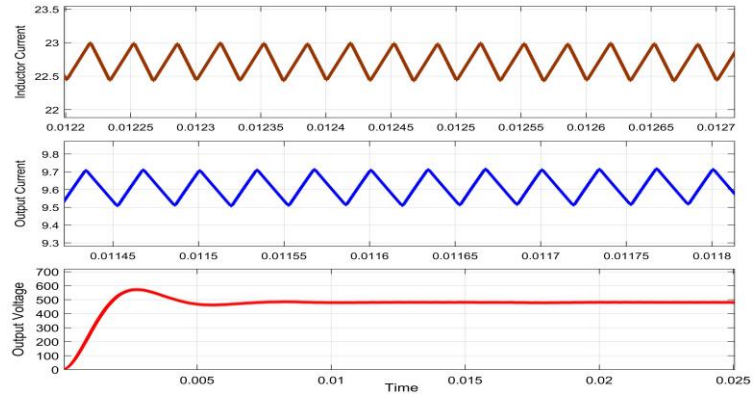

(b)

Fig. 8 Input/output waveforms of BCRC. (a) Waveforms of input current-voltage, and (b) waveforms of inductor current and output current-voltage.

The simulation waveforms of the input/output current-voltage and the inductor current of FBC are depicted in Fig. 9 and Fig. 10.

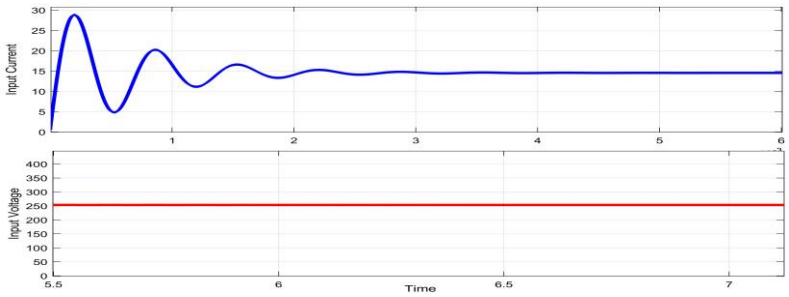

Fig. 9 Simulation input current-voltage waveforms of FBC.

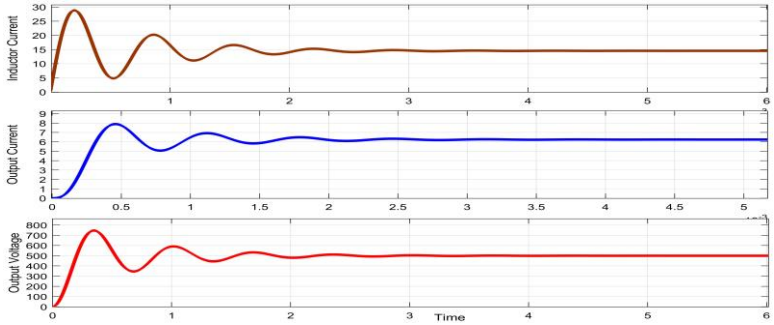

Fig. 10 Simulation waveforms of inductor current and output current-voltage of FBC.

The simulation waveforms of input/output current-voltage and the interleaved inductors current of multi-phase IBC are depicted in Fig. 11 and Fig. 12 respectively.

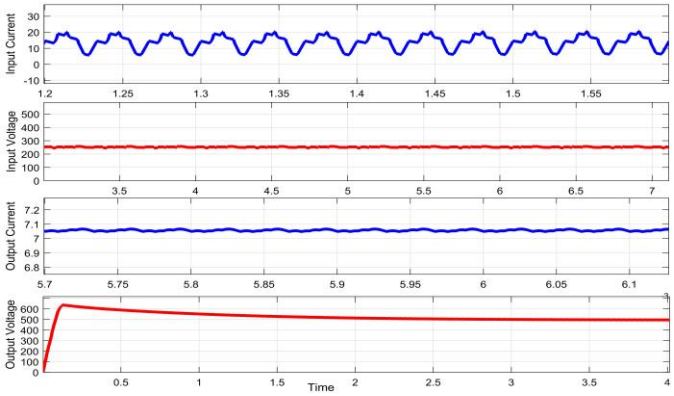

Fig. 11 Input/output current-voltage waveforms of IBC.

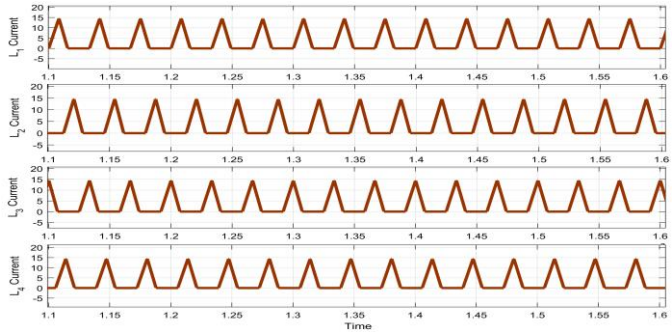

Fig. 12 Waveshapes of the interleaved inductors current of IBC.

The simulation waveforms of the input current-voltage and the inductors current of both ports of MDIBC are depicted in Fig. 13.

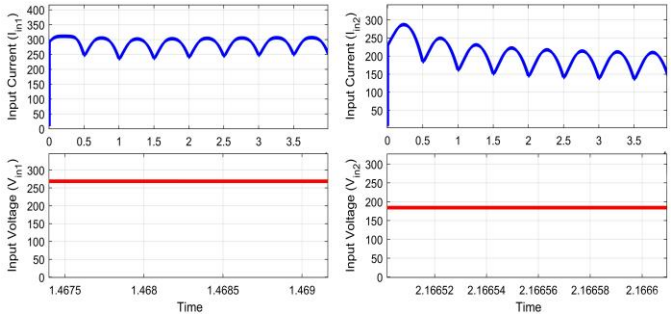

(a)

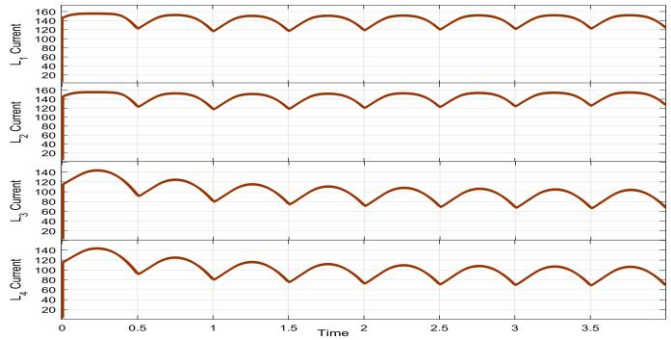

(b)

Fig. 13 Simulation waveforms of the input current-voltage of MDIBC. (a) input current-voltage waveforms, and (b) inductors current waveforms.

Proceedings DOI: 10.21467/proceedings.123
ISBN: 978-81-954993-5-9

Series: AIJR Proceedings
ISSN: 2582-3922

And, the waveforms of the output current-voltage of MDIBC in illustrated in Fig. 14.

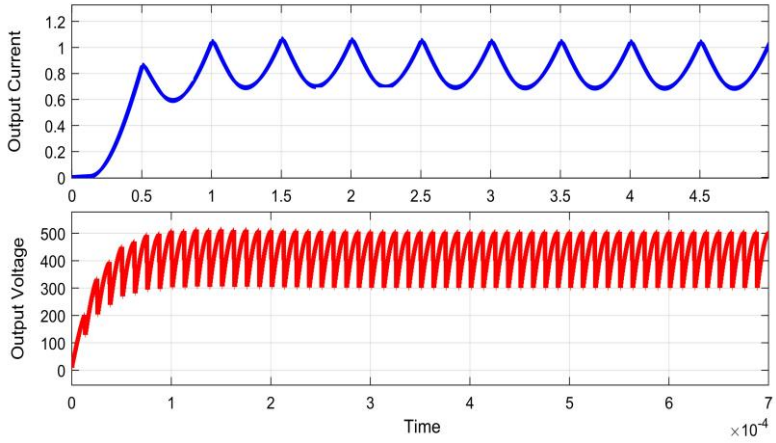

Fig. 14 MDIBC simulation waveforms of output current-voltage.

4 Conclusion

This paper represents a comparative study on isolated and non-isolated power dc-to-dc converters for EVs in which the main power source is PV (photo-voltaic) array module. Although the BCRC is compatible for PV array module based lower-powered vehicular systems due to their high efficiency, smooth starting, soft-switching capability, and lower losses of power switching as well as lower EMI, to conclude, the multi-phase MDIBC for PV based is the best-suited option for both low and high power EVs due to their compact size, multifunctionality, bidirectionality, high efficiency, etc. Therefore, EVs has low GHG emission with many more advanced features than conventional automobiles and with the utilization of solar PV module, the demand of EVs are continuously increasing day by day due to the improvement of the energy efficiency, reliability, and better performance while decreasing the cost.

References

[1] EEA. Total Greenhouse Gas Emissions by Sector (%); European Environment Agency: Copenhagen, Denmark, 2017.
[2] climatecentral.org/gallery/graphics/emissions-sources-2020.
[3] Fontaras, G.; Zacharof, N.-G.; Ciuffo, B. Fuel consumption and CO2 emissions from passenger cars in Europe— Laboratory versus real-world emissions. Prog. Energy Combust. Sci. 2017, 60, 97–131.
[4] Fontaras, G.; Dilara, P. The evolution of European passenger car characteristics 2000–2010 and its effects on real-world CO2 emissions and CO2 reduction policy. Energy Policy 2012, 49, 719–730.
[5] European Commission. Communication from the Commission to the Council and the European Parliament Strategy for Reducing Heavy-Duty Vehicles' Fuel Consumption and CO2 Emissions; European Commission: Brussels, Belgium, 2014.
[6] EEA. CO2 Emission Report; European Environment Agency: Copenhagen, Denmark, 2017.
[7] Chakraborty, S.; Vu, H. N.; Hasan, M. M.; Tran, D. D.; Baghdadi, M. E.; Hegazy, O. DC-DC Converter Topologies for Electric Vehicles, Plug-in Hybrid Electric Vehicles and Fast Charging Stations: State of the Art and Future Trends. Energies 2019, 12(8), 1569.
[8] European Commission. A European Strategy for Low-Emission Mobility, SWD 244 Final; European Commission: Brussels, Belgium, 2016.
[9] Nardone, K.; Curatolo, K. Adaptive Cell Topologies Raise the Bar for DC-DC Converter Performance in EV/HEV Applications.
[10] Averberg, A.; Mertens, A. Analysis of a Voltage-fed Full Bridge DC-DC Converter in Fuel Cell Systems. In Proceedings of the 2007 IEEE Power Electronics Specialists Conference, Orlando, FL, USA, 17–21 June 2007; pp. 286–292.
[11] Al Sakka, M.; Van Mierlo, J.; Gualous, H. DC/DC Converters for Electric Vehicles, Electric Vehicles. Electr. Veh. Model. Simul. 2011.
[12] Kolli, A.; Gaillard, A.; De Bernardinis, A.; Bethoux, O.; Hissel, D.; Khatir, Z. A review on DC/DC converter architectures for power fuel cell applications. Energy Convers. Manag. 2015, 105, 716–730.
[13] Forouzesh,M.; Siwakoti, Y.P.; Gorji, S.A.; Blaabjerg, F.; Lehman, B. Step-Up DC-DC converters: A comprehensive review of voltage-boosting techniques, topologies, and applications. IEEE Trans. Power Electron. 2017, 32, 9143–9178.

[14] Varshney, A.; Kumar, R.; Kuanr, D.; Gupta, M. Soft-Switched Boost DC-DC Converter System for Electric Vehicles using An Auxiliary Resonant Circuit. Inter. J. Emerg. Technol. Adv. Eng. 2014, 4, 845–850.

[15] Park, S.H.; Park, S.R.; Yu, J.S.; Jung, Y.C.; Won, C.Y. Analysis and Design of a Soft-Switching Boost Converter With an HI-Bridge Auxiliary Resonant Circuit. IEEE Trans. Power Electron. 2010, 25, 2142–2149.

[16] Zhang, X.; Qian,W.; Li, Z. Design and Analysis of a Novel ZVZCT Boost Converter With Coupling Effect. IEEE Trans. Power Electron. 2017, 32, 8992–9000.

[17] Han, D.W.; Lee, H.J.; Shin, S.C.; Kim, J.G.; Jung, Y.C.;Won, C.Y. A new soft switching ZVT boost converter using auxiliary resonant circuit. In Proceedings of the 2012 IEEE Vehicle Power and Propulsion Conference, Seoul, Korea, 9–12 October 2012; pp. 1250–1255.

Proceedings DOI: 10.21467/proceedings.123
ISBN: 978-81-954993-5-9

Series: AIJR Proceedings
ISSN: 2582-3922